

Two-Photon Imaging of Brain Pericytes In Vivo Using Dextran-Conjugated Dyes

HAJIME HIRASE, JUDITH CRESO, MALAIKA SINGLETON, PETER BARTHÓ,
AND GYÖRGY BUZSAKI*

*Center for Molecular and Behavioral Neuroscience, Rutgers, State University of New Jersey,
Newark, New Jersey*

KEY WORDS cerebral blood flow; Calcium Green; perivascular cells

ABSTRACT Pericytes in the central nervous system (CNS) are hypothesized to be involved in important circulatory functions, including local blood flow regulation, angiogenesis, immune reaction, and regulation of blood-brain barrier. Despite these putative functions, functional correlates of pericytes in vivo are scarce. We have labeled CNS pericytes using the dextran-conjugated fluorescent calcium indicator Calcium Green I and imaged them in somatosensory cortex of the mouse in vivo. Intracellular calcium concentration in pericytes showed spontaneous surges lasting for several seconds. Furthermore, population bursts of neuronal activity were associated with increased Ca^{2+} signal in a portion of the pericytes. Selective in vivo labeling of pericytes with functional markers may help reveal their physiological function in neuronal activity-associated regulation of local cerebral blood flow. © 2004 Wiley-Liss, Inc.

INTRODUCTION

Pericytes adhere to the outer walls of blood vessels (Rouget, 1873). Although their anatomical features are relatively well described, their physiological function is little understood (Shepro and Morel, 1993; Balabanov and Dore-Duffy, 1998; Thomas, 1999; Rucker et al., 2000). Due to their strategic position, pericytes create an interface between the circulatory system and central nervous system (Hirschi and D'Amore, 1996). Several features of pericytes make them an ideal device for regulating local blood flow according to the demands of neuronal activity. Pericytes contain actin and myosin (Le Beux and Willemot, 1978), the contractile elements in smooth muscle cells, implying the possibility that by contraction and relaxation they may regulate the caliber and/or permeability of blood vessels (Wiederholt et al., 1995; Wagner and Wiederholt, 1996; Stockand and Sansom, 1998). In acutely isolated pericytes from the retina, L-type voltage-gated calcium channels (VGCCs) were recently identified (Sakagami et al., 1999). Importantly, L-type VGCCs are regulated by the extracellular concentration of nitric oxide (NO) (Sakagami et al., 2001), an important volatile messenger in the regulation of local blood flow (Davies, 1995). Two factors have

prevented studying the physiological function of brain pericytes in details. First, no methods are known to label pericytes selectively even in fixed material. Second, their in situ imaging requires high-spatial-resolution methods capable of penetrating into deeper cortical layers, where capillary density is highest (Nakai et al., 1981). We have developed an in vivo method for the reliable and selective labeling of pericytes. After histological verification of the specificity of the labeling method, we imaged them in the living brain using two-photon laser scanning microscopy (2-PLSM) (Denk et al., 1990). This novel in vivo approach opens new possibilities for the detailed examination of their presumed physiological functions.

Grant sponsor: the National Institutes of Health; Grant numbers: NS34994, NS43157, and MH54671 (G.B.); Grant sponsor: Epilepsy Foundation of America (H.H.); Grant sponsor: The Minority Biomedical Research Program (M.S.).

*Correspondence to: György Buzsáki, Center for Molecular and Behavioral Neuroscience, Rutgers, State University of New Jersey, 197 University Avenue, Newark, NJ, 07102. E-mail: buzasaki@andromeda.rutgers.edu

Received 25 March 2003; Accepted 4 June 2003

DOI 10.1002/glia.10295

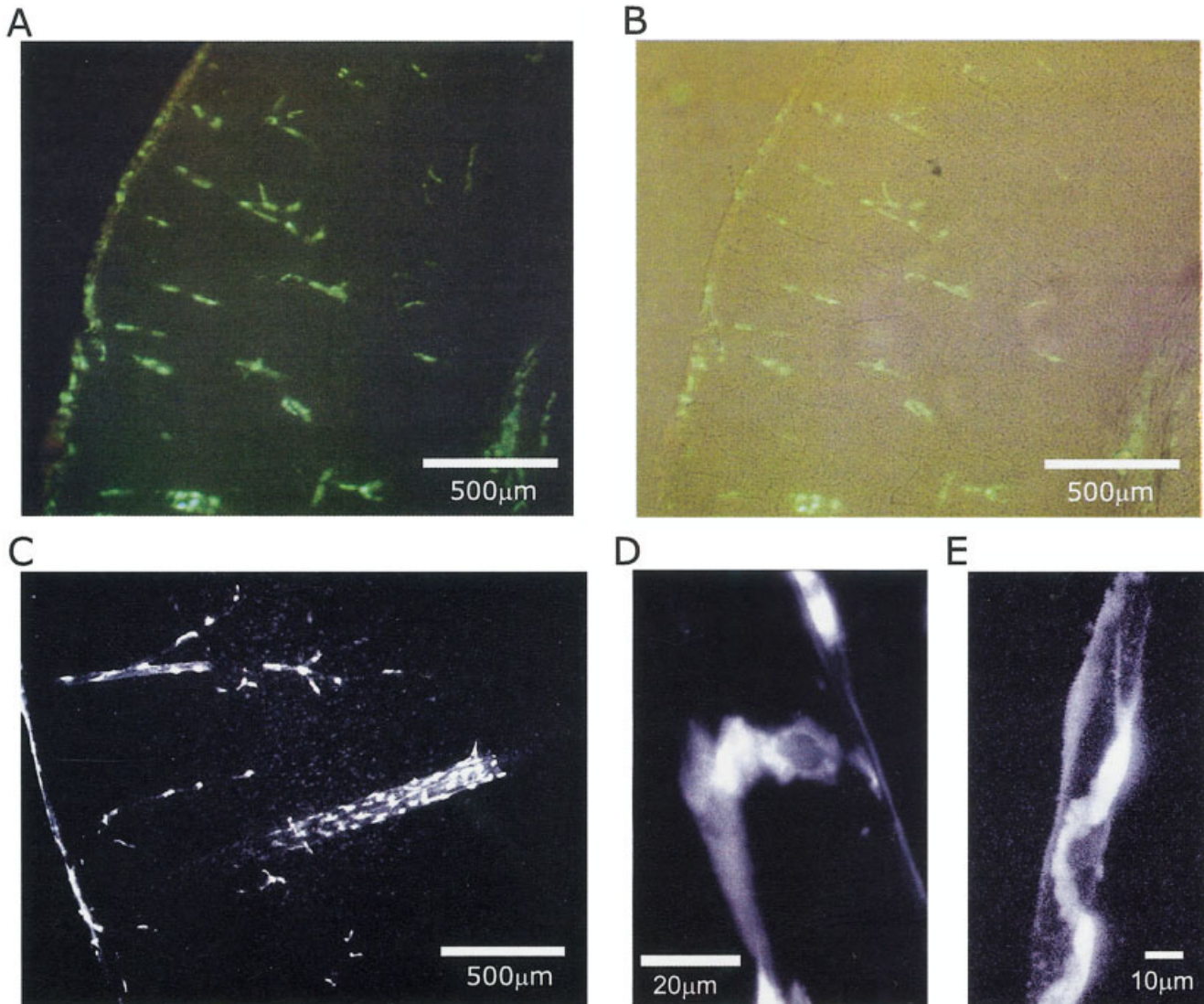


Fig. 1. In vivo loading of dextran-conjugated fluorescent dyes in pericytes. **A:** 100 μm thick fixed brain slice 2.0 mm anterior to the injection site. **B:** Superimposition of phase-enhanced, wide-field microscopy image and the dye-loaded fluorescent image. Note that peri-

cytes are labeled only on a small subset of vessels. **C:** A two-photon scanning of tissue 4.0 mm anterior to the injection site. **D:** Two-photon imaging (magnified) of pericytes around a vein. **E:** 2-PLSM imaging (magnified) of a vessel.

MATERIALS AND METHODS

Twenty-six male and female adult C57BL6 mice (22–32 g) were deeply anesthetized with ketamin/xylazine. Eight of them were used for anatomical examinations only. A small piece of bone was removed from the skull and the dura was opened under microscopic control. FITC dextran (10 kD), Calcium Green I dextran (10 kD) and Fluo-4 dextran (10 kD) were tested. The dyes were dissolved in phosphate-buffered saline (pH 7.4; 5% w/v). A dye-containing glass pipette (tip diameter ~ 100 – $200 \mu\text{m}$) was inserted in the visual cortex (3.2 mm posterior to bregma, 1.5 mm lateral from the midline) at depth 1.0 mm and immediately retracted to the surface. This procedure was repeated five times at the same penetration site. Fast movements were in-

tended to sever some local vessels, which was required for distant cell labeling. Finally, the pipette was placed at depth 1.0 mm and 3 μl of the dye solution was slowly infused (15 min). The scalp was sutured and neomycin was applied around the incision.

One to three days after the dye injection, the animals ($n = 8$) were transcardially perfused with a rinse of saline, followed by 4% paraformaldehyde in 0.1 M phosphate buffer (pH 7.4). The brain was then postfixed in 4% paraformaldehyde for up to 2 days. Slices were cut at 50–100 μm thickness in 0.1 M phosphate buffer using a vibratome.

For in vivo imaging, the mouse was anesthetized again with ketamine-xylazine at least 2 days after the dye injection. A craniotomy (3 mm) was performed above the primary somatosensory area and the dura

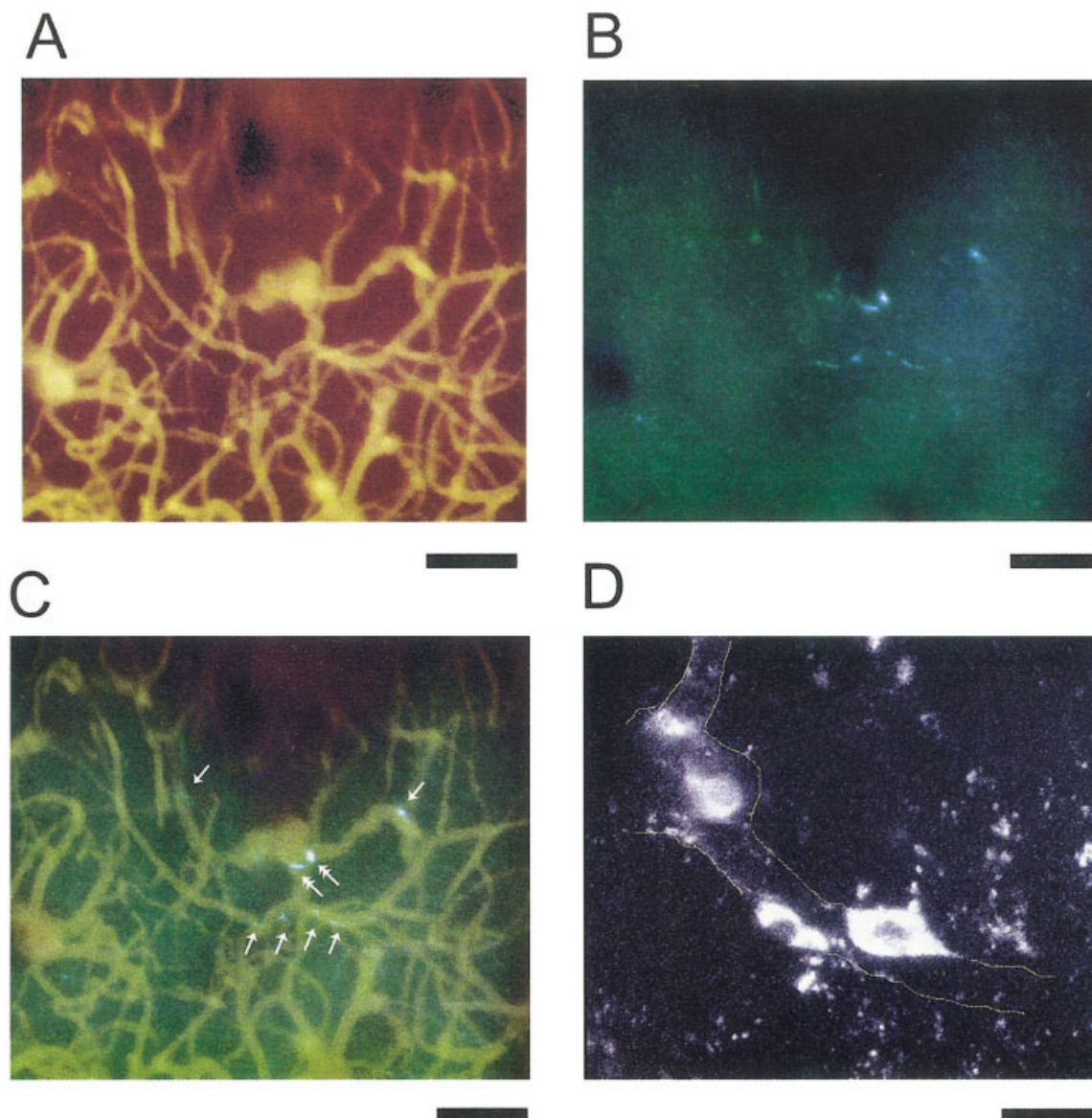


Fig. 2. In vivo imaging of dye-loaded CNS pericytes. **A:** Brain vasculature, visualized by intravenous injection of FITC dextran. **B:** Calcium Green-labeled pericytes, compiled from 200 serial optical sections of $1\ \mu\text{m}$ each. **C:** Overlay of vasculature (FITC) and Calcium Green images. Calcium Green-labeled cells are marked by arrows.

Note their close association with the vasculature. Double arrows denote pericytes at junction points of vessels. **D:** Magnified in vivo imaging of CNS pericytes. Microvessels are outlined with yellow lines. Arrows indicate Calcium Green dextran-labeled pericytes. Scale bar: A, B, and C, $50\ \mu\text{m}$; D, $20\ \mu\text{m}$.

mater was surgically removed. A head frame was fixed with cyanoacrylate cement and the craniotomy was sealed with agarose (1.5% w/v; A-9793 Sigma) in artificial cerebral spinal fluid (ACSF; 125 mM NaCl, 3 mM KCl, 10 mM glucose, 10 mM HEPES, 3.1 mM CaCl_2 , 1.3 mM MgCl_2 , pH 7.4). The electrocardiogram was monitored continuously. Population bursts of cortical neurons (interictal spikes) were induced by inserting a large-tip ($20\text{--}50\ \mu\text{m}$ tip diameter) glass pipette, containing 2 mM bicuculline in 0.9% w/v NaCl, into the deep layers of the somatosensory cortex. This electrode also served to record local field potential and multiple

unit activity. Interictal spikes were reliably observed 10–30 min after the insertion of the pipette.

A custom-made 2-PLSM was constructed similar to that reported by Majewska et al. (2000). Briefly, a Ti:S laser (Mira 800F, Coherent, CA) was pumped by a solid state CW laser (Verdi 8, Coherent) to produce a mode-locked beam (800–830 nm, ~ 100 fs pulse width at 76 MHz). The beam was directed to a modified confocal scan head (Fluoview 300, Olympus, Japan). The fluorescent emission signal was first filtered with an infrared cutting filter (BG-39, Chroma, VT) and band-pass filter for 525 ± 25 nm (HQ525, Chroma) and subse-

quently detected by an external photo-multiplier tube (HC-125-02, Hamamatsu Photonics, Japan). Fluorescent cells were repeatedly scanned with a linearly moving focal point (line scan) at ~ 492 Hz sampling rate. To reconstruct cell morphology, xy scan was taken for every $1 \mu\text{m}$ stack. In some experiments, $50\text{--}70 \mu\text{l}$ of 5% fluorescein isothiocyanate (FITC) dextran (2MD, FD-2000S, Sigma) was injected in the tail vein to visualize the cerebral vasculature (Dirnagl et al., 1992; Kleinfeld et al., 1998; Brown et al., 2001).

RESULTS

Histological Findings

Two to three days after the injection, pericytes accumulated the dextran-conjugated fluorescent dyes in a wide range of brain areas (Fig. 1). Although the cellular uptake of the dye was most prominent around the injection site, the strong background fluorescent intensity obscured the imaging capability around the track. In addition to pericytes, astrocytes and capillary endothelial cells were also labeled in the vicinity ($\sim 300 \mu\text{m}$) of the injection site. All labeled astrocytes appeared to be in close association with vessels with processes (end-feet) in close contact with vessel walls (Peters et al., 1970). Pericytes could be distinguished from astrocytes and endothelial cells by their patchy groupings around vessels (Fig. 1C–E). In contrast to the mixed labeling of different cell types locally, pericytes were selectively loaded at numerous distant cortical sites. Labeling was predominant in the injected hemisphere and spread throughout the anteroposterior direction, including the olfactory bulb and cerebellar cortex. However, occasional pericytes were also observed in the contralateral hemisphere. The labeled pericytes displayed dendritic morphology. Several cytoplasmic processes extended from the cell body and wrapped themselves around the wall of various-size vessels (Peters et al., 1970). Pericyte labeling was sparse and affected only a subset of cells around the vasculature. The intensity and spatial extent of labeling were similar for FITC dextran and Calcium Green I dextran.

In Vivo Imaging of Pericytes

Although the spatial resolution of the imaged cells was less clear in vivo than in the histological material, the distribution of the labeled cells was similar. In the vicinity of the injection site, cells with various morphologies and of high density were observed. In contrast, labeling at distant sites was sparse. Images of labeled putative pericytes were compiled from 200 serial optical sections of $1 \mu\text{m}$ each (Fig. 2). To provide further evidence for the identity of the labeled cells, the cerebral vasculature was visualized by intravenous injection of large-fragment FITC dextran (MW: 2 M Dalton) via the tail vein. Superimposition of the fluorescent images on the vascular image provided further support

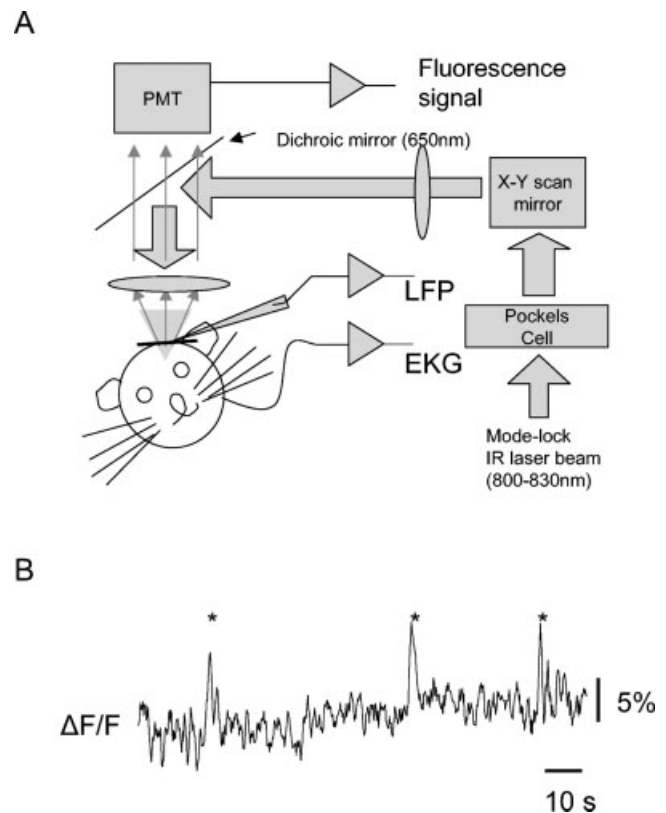


Fig. 3. Two-photon imaging of fluorescence-labeled pericytes in vivo. **A:** Sketch of the imaging setup. The mouse is fixed with a metallic head frame and mounted rigidly under a custom-built two-photon laser-scanning microscope. **B:** An example trace of Calcium Green fluorescence imaging in a pericyte. Sporadic Ca^{2+} surges are marked by asterisks.

for the pericyte identity of the labeled cells (Fig. 2). As observed in the histological sections, pericytes could be imaged several millimeters from the injection site. The best results were observed with $2 \mu\text{l}$ of 5% w/v Calcium Green I dextran. Pericytes were visualized up to $400 \mu\text{m}$ from the pial surface of the cortex in vivo.

After providing anatomical and imaging-based support for the claim that the labeled cells were primarily pericytes, changes in fluorescent intensity of Calcium Green-loaded pericytes were examined (Fig. 3A; $n = 18$ mice). Spontaneous changes of the Ca^{2+} signal in pericytes were not prominent and varied substantially across pericytes. Most pericytes did not show any changes in calcium fluorescence during the observation period (10 min). Nevertheless, in some cells we observed relatively large ($\sim 10\%$ from baseline level) and long-lasting (2–5 s) surges of Ca^{2+} fluorescence that occurred irregularly (Fig. 3B). In a single mouse, a micropipette, containing the GABA_A antagonist bicuculline (2 mM) was inserted into the deep cortical layers to monitor neuronal activity in the barrel cortex. Large-amplitude spikes (mean interspike interval, 3.61 ± 0.72 s) with synchronized unit discharges (interictal spikes) developed 15–60 min after the insertion of the micropipette. The field spikes served as

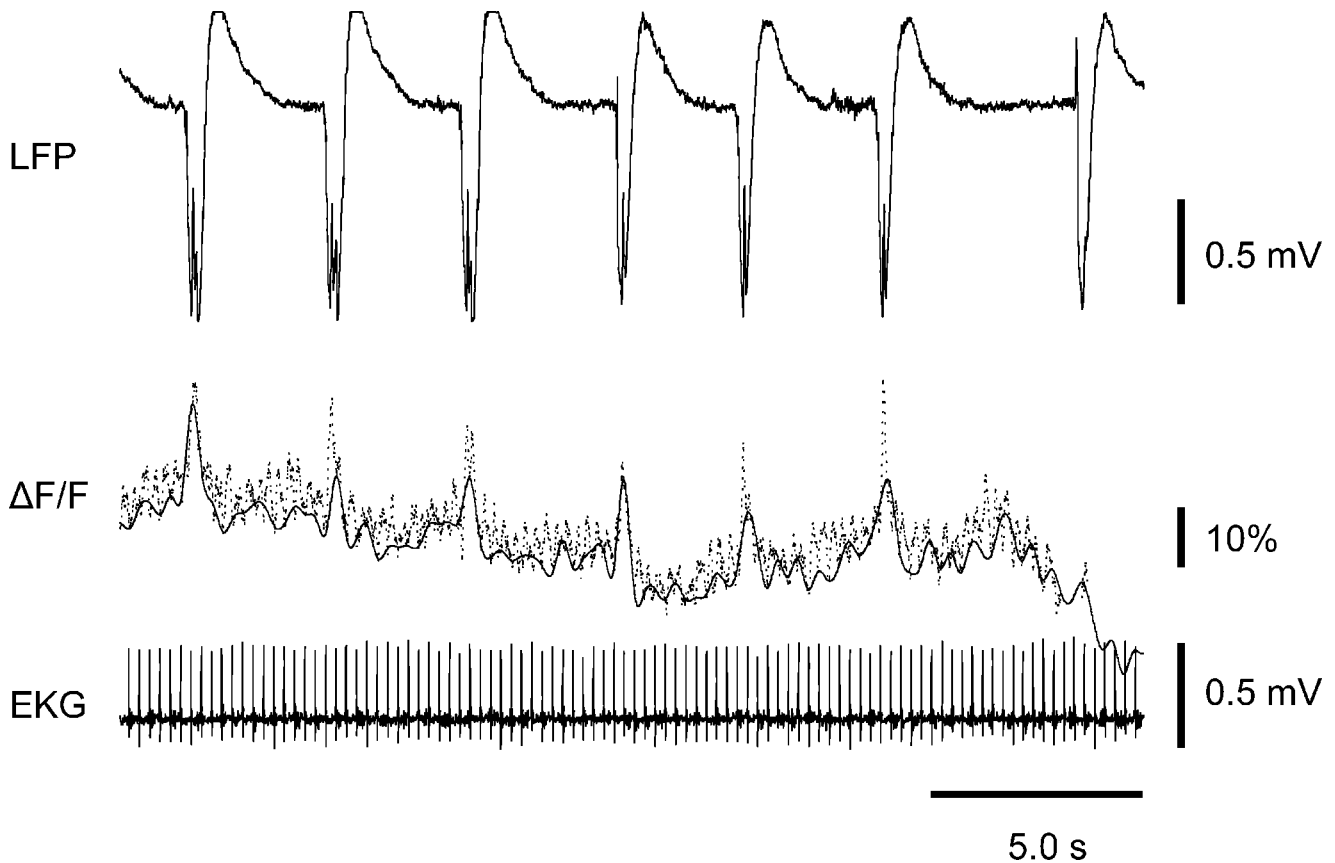


Fig. 4. Neuronal activity-associated increase of Ca^{2+} signal in a pericyte. **Top:** Local field potential (LFP) measured in the vicinity of the imaged area. Neuronal bursts, as reflected by large-amplitude interictal spikes, occurred regularly. **Middle:** Fluorescence intensity change in a Calcium Green-labeled pericyte through time. Dotted line

represents the fluorescence signal before compensation of heart-related brain pulsation. **Bottom:** Heart rate is recorded simultaneously to correct the image intensity artifact due to pulsation of the brain. Note relationship between neuronal bursts and Ca^{2+} changes in the pericyte.

trigger for time averaging of the fluorescent signal. The population discharges were correlated with the fluorescence intensity changes in Calcium Green-loaded pericytes close and distal to the pipette. Figure 4 illustrates Ca^{2+} fluorescence changes in a pericyte in the vicinity of the micropipette. Bursts of neuronal activity induced simultaneous increase of the Ca^{2+} signal. Pericytes imaged several hundred μm from the pipette did not show population burst-associated changes.

DISCUSSION

We described a technique for the selective labeling of pericytes with a functional marker in vivo. The volume injected into the parenchyma likely disrupted local blood vessels, as evidenced by the numerous red blood cells observed around the injection site. Outside the electrode track area, labeling was selective for each of the dextran-conjugated dye examined and we did not see differences in the magnitude of labeling among the different dyes. Labeled pericytes were observed as far as the frontal and occipital cortex and some cells were also observed in the contralateral hemisphere. These

observations suggest that it is the dextran content that is critical for the active uptake by pericytes. Because neither the capillary endothelium nor the smooth muscle surrounding arterioles contained the dye, the findings suggest that pericytes have a special affinity to dextran. Dextran was likely actively accumulated rather than simply transported because labeling was still present for more than 1 week after the injections. These observations indicate that pericytes are specialized to accumulate large-molecular-weight molecules or molecules of certain chemical structures. Independent of the mechanism of dextran uptake, our experiments demonstrate a reliable method for the selective in vivo loading of pericytes with Ca^{2+} sensors.

Numerous unique features of pericytes make them an ideal candidate for mediating between metabolic demands of neurons and local blood supply. The density of pericytes around brain vessels is several-fold higher than in other organs (Frank et al., 1987; Shepro and Morel, 1993). Pericytes, associated with microvessels in the brain, are rich in contractile elements, such as α -SM actin and myosin (Bandopadhyay et al., 2001), and can contract after treatment with histamine, serotonin, angiotensin-2, or ATP (Das et al., 1988;

Kelley et al., 1988; Murphy and Wagner, 1994). Recently, dopaminergic terminals in close proximity of pericytes have been observed in the monkey cortex. Pericytes, like smooth muscle cells, possess excitable membranes and action potential-like Ca^{2+} spikes can be evoked with high concentration of barium or norepinephrine (Wiederholt et al., 1995). Both chemicals strongly depolarize the membrane potential and open L-type VGCCs. In line with the hypothesis that pericytes could play a role in the metabolic regulation of neuronal activity (Hirschi and D'Amore, 1996), Ca^{2+} transients were observed during intense neuronal activity, such as interictal population bursts. Furthermore, spontaneous surges of Ca^{2+} were observed in some pericytes. It is not clear though how these events contribute to vessel control. Increased intracellular Ca^{2+} is expected to lead to muscle contraction in pericytes, and in turn to a decrease in vessel caliber. This scenario is in apparent conflict with the generally accepted view that increased neuronal activity is associated with increased local blood flow (Logothetis et al., 2001). One potential resolution of this apparent conflict is based on the suggestion of the antagonistic action of thoroughfare and exchange capillaries (Hudetz, 1997). According to this view, pericyte contraction may lead to the shunting of thoroughfare capillaries, thereby diverting more blood flow through the exchange vessels. Our preliminary observations suggest that selective labeling of pericytes provides the necessary step for their detailed investigation in the intact brain. Furthermore, these same methods can be applied to other organs such as the retina and kidney, where physiology of acutely prepared or cultured pericytes is well characterized.

REFERENCES

- Balabanov R, Dore-Duffy P. 1998. Role of the CNS microvascular pericyte in the blood-brain barrier. *J Neurosci Res* 53:637–644.
- Bandopadhyay R, Orte C, Lawrenson JG, Reid AR, De Silva S, Allt G. 2001. Contractile proteins in pericytes at the blood-brain and blood-retinal barriers. *J Neurocytol* 30:35–44.
- Brown EB, Campbell RB, Tsuzuki Y, Xu L, Carmeliet P, Fukumura D, Jain RK. 2001. In vivo measurement of gene expression, angiogenesis and physiological function in tumors using multiphoton laser scanning microscopy. *Nat Med* 7:864–868.
- Das A, Frank RN, Weber ML, Kennedy A, Reidy CA, Mancini MA. 1988. ATP causes retinal pericytes to contract in vitro. *Exp Eye Res* 46:349–362.
- Davies PF. 1995. Flow-mediated endothelial mechanotransduction. *Physiol Rev* 75:519–560.
- Denk W, Strickler JH, Webb WW. 1990. Two-photon laser scanning fluorescence microscopy. *Science* 248:73–76.
- Dirnagl U, Villringer A, Einhaupl KM. 1992. In-vivo confocal scanning laser microscopy of the cerebral microcirculation. *J Microsc* 165(Pt 1):147–157.
- Frank RN, Dutta S, Mancini MA. 1987. Pericyte coverage is greater in the retinal than in the cerebral capillaries of the rat. *Invest Ophthalmol Vis Sci* 28:1086–1091.
- Hirschi KK, D'Amore PA. 1996. Pericytes in the microvasculature. *Cardiovasc Res* 32:687–698.
- Hudetz AG. 1997. Blood flow in the cerebral capillary network: a review emphasizing observations with intravital microscopy. *Microcirculation* 4:233–252.
- Kelley C, D'Amore P, Hechtman HB, Shepro D. 1988. Vasoactive hormones and cAMP affect pericyte contraction and stress fibres in vitro. *J Muscle Res Cell Motil* 9:184–194.
- Kleinfeld D, Mitra PP, Helmchen F, Denk W. 1998. Fluctuations and stimulus-induced changes in blood flow observed in individual capillaries in layers 2 through 4 of rat neocortex. *Proc Natl Acad Sci USA* 95:15741–15746.
- Le Beux YJ, Willemot J. 1978. Actin- and myosin-like filaments in rat brain pericytes. *Anat Rec* 190:811–826.
- Logothetis NK, Pauls J, Augath M, Trinath T, Oeltermann A. 2001. Neurophysiological investigation of the basis of the fMRI signal. *Nature* 412:150–157.
- Majewska A, Yiu G, Yuste R. 2000. A custom-made two-photon microscope and deconvolution system. *Pflugers Arch* 441:398–408.
- Murphy DD, Wagner RC. 1994. Differential contractile response of cultured microvascular pericytes to vasoactive agents. *Microcirculation* 1:121–128.
- Nakai K, Imai H, Kamei I, Itakura T, Komari N, Kimura H, Nagai T, Maeda T. 1981. Microangioarchitecture of rat parietal cortex with special reference to vascular “sphincters”: scanning electron microscopic and dark field microscopic study. *Stroke* 12:653–659.
- Peters A, Palay SL, Webster HF. 1970. The fine structure of the nervous system. New York: Harper and Row.
- Rouget C. 1873. Memoire sur le developement de la unique contractile des vesseaux. *Arch Physiol* 79:559–562.
- Rucker HK, Wynder HJ, Thomas WE. 2000. Cellular mechanisms of CNS pericytes. *Brain Res Bull* 51:363–369.
- Sakagami K, Wu DM, Puro DG. 1999. Physiology of rat retinal pericytes: modulation of ion channel activity by serum-derived molecules. *J Physiol* 521(Pt 3):637–650.
- Sakagami K, Kawamura H, Wu DM, Puro DG. 2001. Nitric oxide/cGMP-induced inhibition of calcium and chloride currents in retinal pericytes. *Microvasc Res* 62:196–203.
- Shepro D, Morel NM. 1993. Pericyte physiology. *FASEB J* 7:1031–1038.
- Stockand JD, Sansom SC. 1998. Glomerular mesangial cells: electrophysiology and regulation of contraction. *Physiol Rev* 78:723–744.
- Thomas WE. 1999. Brain macrophages: on the role of pericytes and perivascular cells. *Brain Res Rev* 31:42–57.
- Wagner U, Wiederholt M. 1996. Membrane voltage and whole-cell currents in cultured pericytes of control rats and rats with retinal dystrophy. *Curr Eye Res* 15:1045–1053.
- Wiederholt M, Berweek S, Helbig H. 1995. Electrophysiological properties of cultured retinal capillary pericytes. *Prog Retinal Eye Res* 14:437–451.